Microsolvation of Protonated Methane: Structures and Energetics of $CH_5^+(H_2)_n$

Alexander Witt,* Sergei D. Ivanov, Harald Forbert, and Dominik Marx

Lehrstuhl für Theoretische Chemie, Ruhr-Universität Bochum, 44780 Bochum, Germany

Received: June 19, 2008; Revised Manuscript Received: September 15, 2008

Effects of microsolvating CH_5^+ with up to four H_2 molecules have been investigated in terms of structures and energies. For the smaller complexes, benchmark calculations have been carried out using MP2 and CCSD(T) with basis sets up to aug-cc-pV5Z quality and energies have been extrapolated to the infinite basis set limit. It is found that MP2 calculations using the aug-cc-pVQZ basis set or better yield robust reference data for both structures and energies. More than 30 stationary points including minima and first-order as well as second-order stationary points have been characterized by this method and are discussed in terms of solvation motifs. Finally, the performance of several density functionals has been assessed for this very demanding case. Popular GGA functionals such as BLYP and PBE fail, whereas the TPSS meta-GGA functional captures many structural and energetic aspects of microsolvation satisfactorily.

1. Introduction

Protonated methane, CH_5^+, has been investigated intensively using a host of different experimental and theoretical techniques ever since its reported discovery.[1] A recent review on this interesting molecule is provided in the Introduction of ref 2 where many references to earlier work are collected. The interest in this rather small and, at first glance, seemingly simple molecule is stimulated by various reasons: CH_5^+ is the smallest example of nonclassical carbonium ions featuring unusual multicenter bonding situations due to hypercoordination,[3−5] it is an important reactive intermediate encountered in superacid chemistry,[6] and, last but not least, it plays an important role in astrochemistry.[7−9] After the report of the first high-resolution infrared spectrum[10,11] of the C−H band in 1999 only, a more recent milestone[12] was the recording and assignment of the first broadband infrared spectrum[2,13] of bare CH_5^+, followed by a jet-cooled spectrum[14] of the C−H stretch region.

Moreover, as a particular challenge to theory, the potential energy surface (PES) of CH_5^+ turns out to be extremely shallow. As a result, CH_5^+ was predicted a long time ago,[15] based on early coupled-cluster-like calculations, to exhibit small isomerization barriers such that "one can conclude that at room temperature all the protons are dynamically equivalent".[15] This intriguing phenomenon was later dubbed "hydrogen scrambling", "floppiness", or "fluxionality" in the literature. Therefore CH_5^+ might be considered to be the smallest, but still quite difficult, representative of a whole class of fluxional molecules that exhibit large-amplitude motion. About 20 years later, supportive evidence for this conjecture[15] was given based on more extensive surveys[16−18] using static quantum-chemical calculations leading, finally, to converged relative energies and isomerization barriers provided in ref 19. At about the same time, fluxionality, hydrogen scrambling, and dynamical three-center bonding were indeed demonstrated explicitly using *ab initio* path integral simulations at finite temperatures and could be traced back to quantum-mechanical motion.[20,21] These essential findings, including the interesting consequences of scrambling on site occupations of its isotopologues as reported for the first time in the Response[11] to a Comment, have been confirmed by several different groups using various techniques.[22−31]

Although CH_5^+ itself has been intensively investigated and is now essentially understood, much less attention has been paid to its microsolvated species, $CH_5^+(X)_n$, using initially methane,[32,33] $X = CH_4$, and later molecular hydrogen,[34−37] $X = H_2$, as solvent molecules. Such experiments can be particularly revealing since molecules, which are weakly bound to the CH_5^+ core, are certainly expected to at least perturb the scrambling dynamics. Although the influence of such additional solvating molecules is not yet fully clarified, there is an interesting piece of evidence reported that solvation by as few as three hydrogen molecules slows down scrambling considerably or even stops it completely.[35−37] However, the issue of slowing down versus fully freezing scrambling as a result of solvation is far from being resolved. But when it comes to calculations of such experimentally investigated microsolvation complexes, there is only very scarce information available.[36,38−40]

In this article, we investigate systematically the structural and energetic consequences of microsolvating bare protonated methane, CH_5^+, by several ($n = 1, ..., 4$) H_2 molecules. After a brief summary of the computational methods in section 2, we focus first on the simplest case, $CH_5^+(H_2)$, in section 3. The goal is not only to compare to available data but also to benchmark a low-cost quantum-chemical method, MP2, with different basis sets with respect to much more demanding high-quality coupled cluster calculations. This allows us to judge the ability of MP2 in conjunction with a finite basis set to describe the interaction of H_2 with the bare CH_5^+ core properly. In addition, the performance of popular density functionals of the GGA (generalized gradient approximation) and meta-GGA types is analyzed in detail with respect to this reference quantum-chemical data. As it turns out, the GGA-type functionals used fail to describe CH_5^+ microsolvation of even by only one H_2 molecule, whereas a meta-GGA functional reproduces the reference data quite well. Finally, the economical but still reliable MP2 and meta-GGA electronic structure methods are used for computing structures and energetic properties of larger solvation complexes, $CH_5^+(H_2)_n$ with n up to 4. An extensive set of their isomers is reported and discussed in section 4 followed by a brief summary in section 5.

* Corresponding author, alexander.witt@theochem.rub.de.

10.1021/jp8054069 CCC: $40.75
Published on Web 11/11/2008

2. Computational Details

We performed the wave-function-based calculations using RI-MP2 (resolution of identity Møller−Plesset second-order perturbation theory) as implemented in the Turbomole program package[41] together with the frozen-core approximation. Since it is well known that diffuse functions are crucial for the description of weakly bound complexes, we used the augmented correlation-consistent basis sets of Dunning,[42] in particular aug-cc-pV*X*Z where X = D, T, Q, and 5. The coupled cluster computations, CCSD and CCSD(T), were carried out using the Dalton program package[43] again within the frozen-core approximation together with aug-cc-pV*X*Z basis sets, where X = D, T, and Q.

In addition, basis set extrapolation of MP2 total energies and thus of the resulting binding energies was performed using the MP2/aug-cc-pVQZ and MP2/aug-cc-pV5Z data based on the formula

$$E_{Q5} = E_5^{HF} + \frac{4^3 E_Q^{corr} - 5^3 E_5^{corr}}{4^3 - 5^3} \quad (1)$$

according to the procedure outlined in ref 44. Here, E_5^{HF} is the Hartree−Fock reference energy computed with the quintuple zeta basis set, aug-cc-pV5Z, and E_Q^{corr} and E_5^{corr} are the quadruple and quintuple correlation energies, respectively, obtained from the RI-MP2 calculations. Note that these basis-set-extrapolated energies, E_{Q5}, will be denoted as MP2/aug-cc-pV(Q5)Z energies further down according to the general nomenclature MP2/aug-cc-pV*X*Z.

In addition to quantifying thereby the basis set incompleteness error (BSIE) by approximate extrapolation to the complete basis set (CBS) limit, the basis set superposition error (BSSE) was assessed for a given basis set size. Since the BSSE might be especially significant for weakly bound complexes in conjunction with truly flat PESs (see, e.g., ref 45), the standard counterpoise correction procedure[46] was applied for several selected n = 1 and n = 2 clusters.

The density functional theory (DFT) computations were carried out by means of the CPMD program package[47] using pseudopotentials. In our previous DFT computations and *ab initio* (path integral and classical) simulations of bare CH_5^+, see, e.g., refs 2, 13, 20, and 21, we had found that combining LDA[48] with Becke's gradient correction to exchange,[49] from now on referred to as LDA+B, yields a good representation of the PES in terms of structures, relative energies of stationary points, isomerization barriers, and harmonic frequencies.[2] However, as it turned out in the course of the present investigation, this generalized gradient approximation (GGA) functional fails to describe the rather weak interaction of CH_5^+ with H_2 molecules. Therefore we systematically studied the performance of other density functionals, without aiming at a comprehensive survey at this point. We chose two widely used GGA-type functionals, namely, BLYP[49,50] and PBE[51] as well as the meta-GGA functional TPSS[52] which includes the local kinetic energy density in addition to the local density and its gradient. The DFT calculations of $CH_5^+(H_2)$, $CH_5^+(H_2)_2$, and bare CH_5^+, were carried out in a cubic box with an edge length of 25 au, whereas a 30 au box was used for the larger complexes. We have used a plane wave cutoff of 85 Ry together with norm-conserving pseudopotentials throughout. Troullier−Martins pseudopotentials[53] have been used for BLYP and PBE whereas Giannozzi pseudopotentials (unpublished, but see refs 2, 13, 20, and 21) have been used together with LDA+B and TPSS. The box sizes and the cutoff were confirmed to yield converged binding energies and structural properties.

3. Benchmarking the Methods: $CH_5^+(H_2)$

The goal of this section is to reliably determine the structural and energetic properties of the smallest possible complex, $CH_5^+(H_2)$, to compare the MP2 results to more reliable CCSD and CCSD(T) data, and to check to what extent GGA and meta-GGA type density functionals capture the rather weak intermolecular interactions within the $CH_5^+(H_2)_n$ complex.

3.1. Structures. Altogether 45 initial configurations of the H_2 molecule covering the whole space around the CH_5^+ core (taking symmetry into account) were used for structure optimization. As it is well-known that MP2 is able to describe structures of such weakly bound complexes quite well,[54,55] we used this method to perform structure relaxations. All optimizations were started using the economical aug-cc-pVTZ basis, whereas the final refinement of structures was carried out with the aug-cc-pV5Z basis set. As a result of this search, four minima, seven first-order stationary (saddle) points, and four second-order stationary points on the PES as presented in Figure 1 were finally found as confirmed by stability analysis; note that this search is by no means comprehensive but should only serve to provide us with a reasonable database for benchmarking. The global minimum of bare CH_5^+ has C_s symmetry which remains true for the solvated case as well (see structure **6** in Figure 1). Note that there exist two C_s stationary points (see for instance ref 2), the eclipsed one being the global minimum whereas the staggered C_s structure is a saddle point to internal rotation which lies only about 0.1 kcal/mol above the global minimum.[19] In the present investigation we focused on eclipsed conformations. Therefore, there is one symmetry plane σ_h which contains three hydrogen atoms $H^{(1)}$, $H^{(2)}$, and $H^{(3)}$, where we number the five hydrogen atoms in the CH_5^+ core and refer to atoms in the solvating H_2 molecule(s) by latin letters as indicated in Figure 1. $H^{(1)}$ and $H^{(2)}$, which are about 1 Å apart from each other, form what is traditionally referred to as the "moiety" and together with carbon they participate in a three-center two-electron bond.[21] Atoms $H^{(3)}$, $H^{(4)}$, and $H^{(5)}$ constitute with the carbon the so-called "tripod"; note that the charge state of these conceptual fragments is obviously not specified hereby. The hydrogen atoms of the tripod are now classified relative to the symmetry plane σ_h. Thus, $H^{(3)}$ is called "in-plane", while $H^{(4)}$ and $H^{(5)}$ are referred to as "out-of-plane". Note that hydrogen atoms in the moiety also differ: $H^{(2)}$ is considered to be "inside" the moiety, since it is placed between $H^{(1)}$ (the "outside" atom in the moiety) and the in-plane hydrogen $H^{(3)}$.

On the basis of such a core structure, several motifs to attach solvating H_2 molecules can be imagined. Clearly, there exist several expected sites which can be occupied by H_2, namely, it can be attached to one of the five hydrogen atoms and it is conceivable that it is attached simultaneously to two hydrogens of the moiety or under the tripod. Furthermore, at each individual site, the hydrogen molecule can be oriented perpendicular to the symmetry plane σ_h, it can be parallel to it, or it can be aligned along a $C-H^{(\alpha)}$ axis where $H^{(\alpha)}$ is one of the five hydrogen atoms of the CH_5^+ core. Using our search protocol, we have first of all reproduced all structures discussed in ref 39, i.e., structures **1**, **2**, **4**, **6**−**9**, **11**, **14**, and **15**, without specifying them explicitly. In addition we found several interesting new structures, namely, structures **3**, **5**, **10**, **12**, and **13**. As expected, we observed that the relaxation procedure is very sensitive with respect to the initial conditions. We group most of the structures according to the sites occupied by the attached H_2 molecule as explained above. In particular, in structures **1**−**3** the molecule is attached to $H^{(1)}$ in all three possible orientations. However, normal mode analysis shows that only structure **1**, in which the

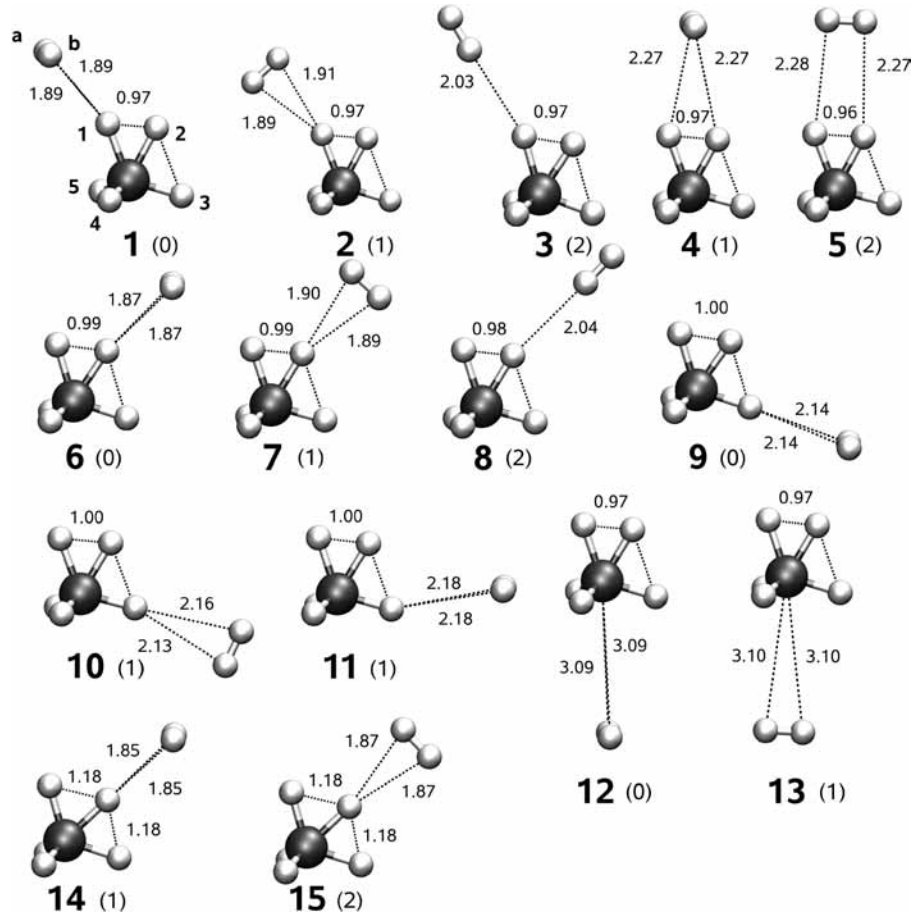

Figure 1. Stationary points of the $CH_5^+(H_2)$ complex. The values in parentheses following the number of the structure denote the number of imaginary frequencies; structure **6** corresponds to the global minimum. Note: the lines are not intended to denote chemical bonds but only to guide the eye.

H_2 molecule is perpendicular to the symmetry plane, is a minimum. That turns out to be a rather general rule: perpendicular orientation of the hydrogen molecule to the symmetry plane often leads to a minimum; see structures **1**, **6**, **9**, and **12**.

Structure **2** is a saddle point, which is the transition state for the rotation of H_2, and structure **3** is a second-order stationary point. In addition, the three orientations akin to structures **1**−**3** for $H^{(1)}$ are found for $H^{(2)}$ as well; see structures **6**−**8**. In structures **4** and **5**, the hydrogen molecule is attached to the moiety either perpendicular to the mirror plane or parallel to it, respectively.

Structure **4** is the transition state between the two minima structures **1** and **6** associated with the outside and inside moiety hydrogen atoms, whereas structure **5** is a second-order stationary point. Note that a possible third orientation, where H_2 is attached to the moiety in the plane but pointing perpendicular to the $H^{(1)}-H^{(2)}$ axis, was not observed. In structures **9** and **10** the hydrogen molecule is attached to the in-plane atom $H^{(3)}$ and is either perpendicularly or parallelly oriented with respect to the symmetry plane. Again, the perpendicular orientation is a minimum and the parallel orientation is a saddle point. Note that the orientation of structures **9** and **11** is identical, but in structure **11** the angle between the $C-H^{(3)}$ and the intermolecular H_2 bond differs from structure **9**. Thus structure **11** is probably the transition state between structures **9** and **6**. Finally, we found structures **12** and **13**, where the H_2 molecule is located under the tripod, roughly perpendicular to its pseudo-$C^{(3)}$ axis. Again, perpendicular orientation to the symmetry plane yields a minimum (structure **12**), while parallel orientation (structure **13**) corresponds to the rotational transition state. It is worth noting that we could not stabilize minima where the molecule is attached to the CH_5^+ core via the out-of-plane hydrogens, $H^{(4)}$ or $H^{(5)}$. For such starting structures, optimization always resulted in a moiety rotation and ended up with structure **9** or **11**. However, it might well be that such minima exist as well but that they escaped our simple protocol of searching the PES.

In addition to these minima, we tried to find possible transition states for the hydrogen scrambling within the CH_5^+ core itself in the presence of one solvating hydrogen molecule. Two putative candidates are structures **14** and **15** both featuring C_{2v} symmetry. However, vibrational analysis shows that only structure **14** is a true transition state for scrambling in **6** whereas structure **15** is again a second-order stationary point and seems to exhibit a scrambling event with respect to transition state **7**. Concluding this part, we found a set of well-defined structures that represent both minima and stationary points and display furthermore a large variety of qualitatively different solvation motifs. This structural database should be sufficient in order to scrutinize practical electronic structure methods with respect to accurate energies from coupled cluster calculations, which are too demanding to be carried out systematically for larger systems in particular when it comes to structure search and optimization.

3.2. Energetics. Before we proceed to analyze the relative stabilities of these 15 stationary points which characterize important parts of the 18-dimensional PES of $CH_5^+(H_2)$, we examine the accuracy of the MP2 approximation first. For this purpose, we compare the binding energies to coupled cluster

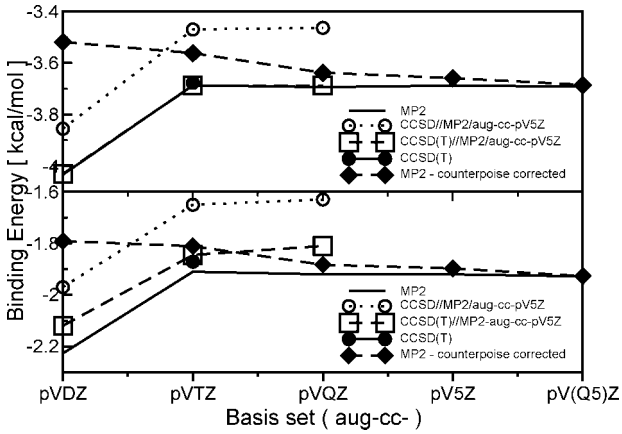

Figure 2. Binding energies of structure **6** (upper graph) and structure **9** (lower graph) for the $CH_5^+(H_2)$ complex with respect to basis set computed using various methods. "MP2" data (solid lines) are fully optimized using the reported basis set, "CCSD//MP2/aug-cc-pV5Z" and "CCSD(T)//MP2/aug-cc-pV5Z" data (dotted and dashed lines/open squares, respectively) are single point calculations based on the optimized MP2/aug-cc-pV5Z structures, "CCSD(T)" data at the aug-cc-pVTZ basis (filled circles) correspond to full optimization using this basis set and method, and "MP2 - counterpoise corrected" data (diamonds) are counterpoise corrected (see text) using the reported basis set.

results for two representative structures: the global minimum which is structure **6** and the weaker bound complex **9**; see Figure 1. Single-point calculations were carried out with CCSD and CCSD(T) to obtain the energy as a function of basis set size using the optimized MP2/aug-cc-pV5Z structures. Binding energies were then computed as usual from $\Delta E = E(CH_5^+(H_2)) - E(CH_5^+) - E(H_2)$ with respect to the isolated fragments CH_5^+ and H_2, which were separately optimized using the same setup as for $CH_5^+(H_2)$. The results of these systematic studies are summarized in Figure 2 where we compare the MP2 data to the coupled cluster data. Furthermore, using the same figure one can assess the convergence with respect to the basis set size. The basis set limit is approximated by the extrapolation (Q5) given in eq 1. Full structure optimization was also carried out at the CCSD(T) level for structures **6** and **9** using the medium-sized aug-cc-pVTZ basis set in order to check the influence of relaxation on the binding energy.

Several crucial insights can be gained from these tests. First, the aug-cc-pVDZ basis set turns out to be too small to produce binding energies of acceptable quality. The counterpoise-corrected binding energies for the aug-cc-pVDZ basis set are noticeably closer to the aug-cc-pV(Q5)Z CBS values compared to the uncorrected values subject to BSSE, but still these relative energies are unsatisfactory in view of a sizable BSIE; see Figure 2. But already the aug-cc-pVTZ basis set improves the results considerably and yields much smaller differences in binding energies for both structures with reference to the (Q5) extrapolated CBS limit. Still, the BSIE is noticeable when comparing the counterpoise corrected aug-cc-pVTZ data to the (Q5) extrapolated binding energies, whereas the BSIE becomes negligible for larger basis sets in view of the convergence of the BSSE corrected aug-cc-pVQZ and aug-cc-pV5Z values. In the latter cases the BSSE amounts to only 2% and 1%, respectively, to the CBS data; see Figure 2. This suggests that error compensation of BSSE and BSIE works effectively using these basis sets in the particular bond strength regime that is relevant to the system of interest. We thus conclude that basis sets of aug-cc-pVQZ or higher quality are suitable for a proper description of the energetics of these systems by means of the MP2 method.

TABLE 1: Binding Energies in kcal/mol for Structures 1−15 of Figure 1 Computed with MP2/aug-cc-pV5Z

	1	**2**	**3**	**4**	**5**
binding energy	−3.34	−3.25	−0.50	−2.64	−2.42
	6	**7**	**8**	**9**	**10**
binding energy	−3.69	−3.47	−0.61	−1.92	−1.84
	11	**12**	**13**	**14**	**15**
binding energy	−1.85	−1.21	−1.19	−3.29	−3.04

Second, the CCSD(T) binding energies turn out to be quite close to the MP2 data independently from the basis set choice, whereas CCSD data seem to systematically underestimate binding energies by about 0.2 kcal/mol. Finally, it seems that single-point CCSD(T) computations based on the MP2-optimized structures mentioned above yield results that are already fairly close to the ones obtained by fully relaxed CCSD(T) calculations as checked by using the aug-cc-pVTZ basis. Hence, we conclude that fully relaxed MP2/aug-cc-pVQZ or MP2/aug-cc-pV5Z data can safely serve us as reference values to investigate all isomers and to assess other electronic structure methods. The MP2/aug-cc-pV5Z method has therefore been used to compute the binding energies of all structures collected in Figure 1; see Table 1. It turns out that the H_2 molecule prefers to be attached to the moiety atoms instead of those in the tripod. Indeed, the hydrogen molecule attached to $H^{(2)}$ yields the global minimum structure **6** (−3.69 kcal/mol), which is qualitatively consistent with the conclusions drawn in ref 39. The binding energy of the local minimum given by structure **1** where the solvating hydrogen molecule is attached to the other site of the moiety ($H^{(1)}$) is approximately only 0.3 kcal/mol higher in energy than the global minimum. The H_2 molecule solvating $H^{(3)}$, see structure **9**, turns out to be bound weaker by nearly a factor of 2 compared to the global minimum. And finally the last minimum observed where H_2 solvates the tripod from below, i.e., structure **12**, features the weakest binding within the ensemble of generated minima, its binding energy being just −1.21 kcal/mol.

As we already pointed out previously, all minimum structures have the hydrogen molecule attached perpendicularly to the symmetry plane. Orientations parallel to the symmetry plane (namely, structures **2**, **7**, **10**, and **13**) yield rotational transition states which are only a few percent higher in energy than the corresponding minima as expected. Structure **4** is the transition state between isomers **1** and **6**, and structure **15** can be considered as the rotational transition state on top of the scrambling transition state (structure **14**). The rotational transition state for structure **11**, which itself is the transition between structures **9** and **6**, has not been found. Interestingly, the saddle point structure **11** has nearly the same energy as the minimum structure **9**.

Another interesting finding is that the binding energy of H_2 in the transition state structure of $CH_5^+(H_2)$, **14**, is only about 0.39 kcal/mol higher than the one of the global minimum **6**. This should be compared to the scrambling barrier in bare CH_5^+, namely, the energy difference between its eclipsed C_s minimum and the corresponding C_{2v} transition state, where we find 0.53 kcal/mol using the same method and basis set, i.e., MP2/aug-cc-pV5Z (see data collected in Table 2). Note that the CCSD(T) value for the scrambling barrier within $CH_5^+(H_2)$ (obtained as the energy difference between structure **14** and **6** using

TABLE 2: Binding Energies of $CH_5^+(H_2)$ in kcal/mol for Structures 6, 9, and 12 in Figure 1 Computed with MP2, CCSD(T), HF, and DFT Using Different GGA Functionals (LDA+B, BLYP, PBE) and One meta-GGA Functional (TPSS)[a]

				scrambling barrier in	
method	**6**	**9**	**12**	CH_5^+	$CH_5^+(H_2)$
MP2	−3.69	−1.92	−1.21	0.53	0.39
CCSD(T)	−3.68	−1.83	−1.23	0.88	0.69
HF	−1.83	−0.30	−0.65	2.35	1.96
LDA+B	−2.48	−0.94	−0.29	0.64	0.51
PBE	−4.87	−	−1.13	0.00	−0.14
BLYP	−3.69	−1.79	−0.56	0.25	0.16
TPSS	−4.27	−1.93	−0.97	0.58	0.35

[a] The coupled cluster results are CCSD(T)/aug-cc-pVTZ//MP2/aug-cc-pV5Z data whereas all other results are based on fully optimized structures using the given method. The scrambling barriers of bare CH_5^+ and $CH_5^+(H_2)$ (defined as the energy difference between structures **6** and **14**) are reported using the same methods.

TABLE 3: Important Structural Parameters of $CH_5^+(H_2)$, Structures 6, 9, and 12, Computed with Different Electronic Structure Methods As Explained in Table 2

structure/ method	$d(C-H^{(a)}/C-H^{(b)})$ (Å)	$d(H^{(a)}-H^{(b)})$ (Å)	d (moiety) (Å)	angle $H^{(1)}-C-H^{(2)}$	angle $H^{(2)}-C-H^{(3)}$
6/MP2	3.04/3.04	0.74	0.99	49.6	74.3
6/CCSD(T)	3.06/3.06	0.75	0.96	47.5	76.1
6/LDA+B	3.05/3.07	0.75	0.98	48.3	76.6
6/PBE	3.00/3.00	0.76	1.16	59.1	68.4
6/BLYP	3.02/3.04	0.76	1.04	51.5	74.7
6/TPSS	3.04/3.05	0.76	1.00	49.7	75.3
9/MP2	3.24/3.24	0.74	1.00	51.0	73.6
9/CCSD(T)	3.27/3.27	0.75	0.97	48.0	76.3
9/LDA+B	3.28/3.22	0.74	1.01	52.5	75.8
9/PBE	−	−	−	−	−
9/BLYP	3.24/3.26	0.75	1.10	56.2	72.0
9/TPSS	3.22/3.22	0.75	1.03	51.7	74.5
12/MP2	3.09/3.09	0.74	0.97	48.6	76.2
12/LDA+B	3.10/3.17	0.74	0.96	47.2	78.5
12/PBE	3.13/3.18	0.76	1.15	59.3	69.5
12/BLYP	3.11/3.14	0.75	1.01	50.2	76.6
12/TPSS	3.10/3.20	0.74	0.97	47.9	77.6

CCSD(T)/aug-cc-pVTZ//MP2/aug-cc-pV5Z data) is 0.69 kcal/mol whereas it is 0.88 kcal/mol for bare CH_5^+ using the same method. This shows that MP2 underestimates the scrambling barrier somewhat but in a seemingly systematic manner thereby reproducing the CCSD(T) trend. Thus, surprisingly, the possibility exists that attaching one H_2 molecule might enhance hydrogen scrambling in the CH_5^+ core by decreasing the relative energy of the corresponding saddle point by about 0.2 kcal/mol as a result of microsolvation. However, it is unclear at this level of theory how the modified scrambling energetics would influence the scrambling dynamics within $CH_5^+(H_2)$. Taken together, the analysis of minima and saddle points substantiates the point that $CH_5^+(H_2)$ produces a rich and flat PES featuring not only low-lying transition states delineating possible scrambling pathways but also several energetically preferred detachment channels, $CH_5^+(H_2) \rightarrow CH_5^+ + H_2$.

3.3. Assessing Density Functionals. In the previous section we already demonstrated that MP2/aug-cc-pV5Z as well as MP2/aug-cc-pVQZ calculations provide reliable reference values for structural and energetic properties of $CH_5^+(H_2)$. At this stage we are in a position to compare the performance of various density functionals with respect to these reference values. Since we are interested in microsolvation and its possible impact on the scrambling dynamics, we rate the "quality" of a given functional based on three important criteria, namely, the ability to reproduce structures, binding energies, and scrambling barriers. The latter are obtained for CH_5^+ and $CH_5^+(H_2)$ in terms of the energy difference between the C_s and C_{2v} structures. Here we have chosen to test functionals on the structures **6**, **9**, and **12** as shown in Figure 1, since they represent more and less strongly bound complexes, respectively. On the basis of the data shown in Table 2, one again sees that the MP2 binding energies are close to the CCSD(T) results and that MP2 consistently underestimates scrambling barriers both for bare CH_5^+ and for the $CH_5^+(H_2)$ complex by about 0.3 kcal/mol. The barrier in bare CH_5^+ is determined to be 0.82 kcal/mol based on CCSD(T)-R12 data where a large basis set was used and the best estimate is 0.8 kcal/mol according to ref 19. We note that our CCSD(T) value listed in Table 2 is close to this result. We want to point out that the Hartree−Fock (HF) binding energies are much too low whereas the scrambling barriers are far too high, which renders this very economical method useless for this problem. Clearly, the best values for the scrambling barrier of bare CH_5^+ using DFT are obtained with LDA+B, as employed in several earlier dynamical simulation studies.[2,13,20,21] However, we observe that the LDA+B functional underestimates binding energies for all complexes under consideration. This effect is especially pronounced for the weakly bound microsolvation complex **12**. BLYP on the other hand yields nearly perfect results for the global minimum and the intermediate structure. However, the energy of the weakly bound complex is underestimated by a factor of 2. Unfortunately BLYP cannot reproduce both scrambling barriers properly: they are dramatically underestimated. PBE even fails to find structure **9**, since optimization led to structure **1** in Figure 1. The energy of the global minimum is overestimated in this case, while the result for the weakly bound complex is acceptable. However, PBE shows no scrambling barrier at all since the corresponding energy is negative. Consequently, PBE is not a functional of choice for the systems studied here. The TPSS meta-GGA functional overestimates the stability of the global minimum somewhat, whereas the energies for the other two structures are decent and scrambling barriers are of MP2 quality even in the microsolvated $CH_5^+(H_2)$ complex.

Finally, we compare structural properties for the chosen structures using all functionals with the MP2/cc-aug-pV5Z reference data; the CCSD(T)/cc-aug-pVTZ structures **6** and **9** are included in order to demonstrate how close they are to the MP2 structures. The data compiled in Table 3 shows that nearly all density functionals are able to reproduce the MP2 structures of $CH_5^+(H_2)$ quite well, with the noticeable exception of the PBE functional. With PBE, both the $H^{(1)}-H^{(2)}$ distance in the moiety and the moiety angle ($H^{(1)}-C-H^{(2)}$) in structures **6** and **12** are unacceptably large.

With this detailed comparison we have shown that despite being best to reproduce scrambling barriers in both bare and microsolvated CH_5^+, LDA+B cannot be used to study microsolvation since the binding energies it yields are unacceptably low. BLYP underestimates the scrambling barriers considerably, whereas PBE fails to provide correct structures. The TPSS meta-GGA functional on the other hand leads to acceptable binding energies as well as structures of $CH_5^+(H_2)$ and scrambling barrier of the CH_5^+ core. Its only deficiency is that it somewhat underestimates the scrambling barrier for $CH_5^+(H_2)$. However, TPSS still reproduces the important trend that the scrambling barrier of the $CH_5^+(H_2)$ complex is lower than that in the bare species. Thus, we are left with the conclusion that TPSS is the

only functional within the studied set that closely satisfies all three of the aforementioned quality criteria.

4. Assessing Microsolvation Effects: $CH_5^+(H_2)_n$

4.1. The Smallest Case: $CH_5^+(H_2)_2$. On the basis of this rather comprehensive investigation of $CH_5^+(H_2)$ we have demonstrated that MP2/cc-aug-pV5Z data can be used to produce reliable structures and energies. One could argue that this will also hold for larger complexes since we expect to find H_2 molecules at approximately the same sites as in $CH_5^+(H_2)$ while $H_2 \cdots H_2$ interactions in $CH_5^+(H_2)_n$ should be fairly weak. Since the latter point might be questioned in view of the overall weak interactions that govern the structures of these microsolvated complexes, we again used single-point CCSD(T) calculations to compare explicitly to the MP2 binding energies of $CH_5^+(H_2)_2$. These calculations should serve as reference data to double check the conjecture that MP2 also describes such larger complexes properly. We constructed structures for the complex $CH_5^+(H_2)_2$ in two fashions: either we combined minima of the $CH_5^+(H_2)$ complex or we used the same procedure as mentioned in the previous section to obtain new minima. Once we reached a stationary point on the PES, we performed vibrational analysis to check whether this stationary point is a minimum, a transition state or a higher-order stationary point. The convergence with respect to the basis set was done following the same protocol as was established for $CH_5^+(H_2)$. Again, the BSSE was estimated to be approximately 2% and at most 1% of the binding energies for an aug-cc-pVQZ and an aug-cc-pV5Z basis set, respectively. This indicates that the BSSE, indeed, can be neglected when using these basis sets together with the MP2 approximation on the binding energy scale that is relevant to microsolvation of CH_5^+. We show a representative set of all so far obtained stable isomers in Figure 3; again we note that this is by far not a comprehensive survey. As before, typically more than one initial structure resulted in the same optimized structure. Most of the minima found can be constructed by a combination of two known minima of $CH_5^+(H_2)$. Indeed, structures **1** and **2** from Figure 3 can be considered as combinations of structures **1** and **6** and structures **6** and **9** from Figure 1, respectively. Analogously, structures **3** and **5** from Figure 3 can be constructed out of structures **1** and **9** and **6** and **13** of $CH_5^+(H_2)$, respectively. Although the $CH_5^+(H_2)$ complex **13** is not a minimum, but a rotational transition state, it nevertheless contributed to the stable structure in $CH_5^+(H_2)_2$. The two structures **4** and **6** are interesting because new positions are occupied there by the solvating H_2 molecules. In these structures the two hydrogen molecules are found to be attached to one (**4**) or to both (**6**) of the two out-of-plane hydrogen sites, $H^{(4)}$ and $H^{(5)}$, which is a motif that was not stable in the $CH_5^+(H_2)$ case. This might indicate that the moiety rotation observed in the case of $CH_5^+(H_2)$ is hindered in the presence of an additional hydrogen molecule, i.e., that this is a steric effect.

Clearly, the PES is even more complicated in this case and additional structural motifs are found. It is expected that many more minima could be located, which is however not the purpose of this study. In Table 4 we present the binding energies obtained as the total energy difference of the complex with respect to all fully relaxed fragments, i.e., $\Delta E = E(CH_5^+(H_2)_n) - E(CH_5^+) - nE(H_2)$, $n = 2$. Again, we used various methods to obtain these binding energies, namely, HF, MP2, CCSD(T), and DFT with all considered functionals (LDA+B, BLYP, PBE, and TPSS). First of all, the MP2 binding energies are fully verified by the CCSD(T) numbers as conjectured. The second observation is that HF underestimates all binding energies dramatically thus confirming its failure already found for $CH_5^+(H_2)$. Moreover, the trend of relative stabilities is not reproduced by HF, namely, structure **2** is less stable than structures **3**−**5** which in fact should be the opposite according to the MP2 or CCSD(T) reference results. This confirms that electron correlation is crucial for the investigated systems.

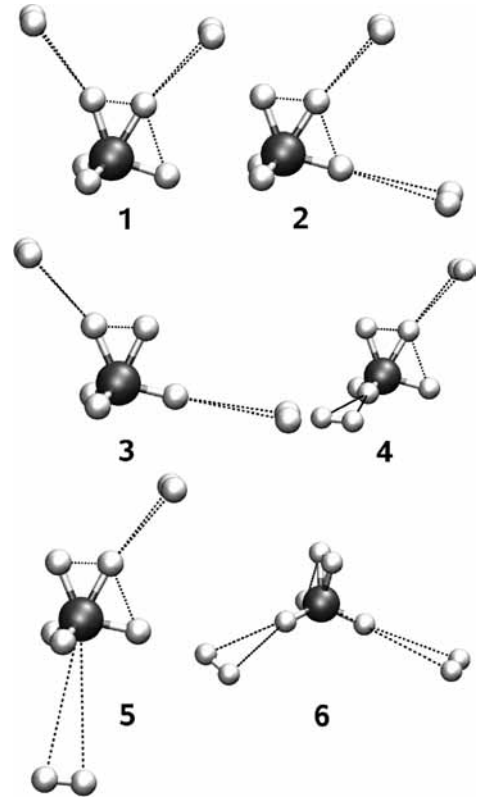

Figure 3. Energetic minima of the $CH_5^+(H_2)_2$ complex. Note: the lines are not intended to denote chemical bonds but only to guide the eye.

TABLE 4: Binding Energies of $CH_5^+(H_2)_2$ in kcal/mol Computed with MP2/aug-cc-pV5Z in Comparison to CCSD(T)/aug-cc-pVTZ//MP2/aug-cc-pVQZ and DFT Functionals

method	1	2	3	4	5	6
MP2	−6.71	−5.52	−5.04	−4.99	−4.80	−2.71
CCSD(T)	−6.85	−5.50	−5.16	−5.07	−4.88	−2.85
HF	−3.60	−2.06	−2.48	−2.45	−2.43	−1.24
LDA+B	−4.35	−3.33	−3.10	−3.01	−2.66	−1.18
PBE	−8.33	−	−6.50	−6.36	−5.87	−3.28
BLYP	−6.29	−5.12	−4.77	−4.60	−4.12	−2.02
TPSS	−7.46	−5.99	−5.57	−5.50	−5.14	−2.64

Furthermore, all DFT functionals fully reproduce the trend of relative stabilities, which are continuously decreasing from structures **1** to **6** according to Table 4. However, as already noticed for the smaller cluster $CH_5^+(H_2)$, LDA+B underestimates all binding energies. BLYP again slightly underestimates all binding energies but performs better than LDA+B overall. The PBE functional overestimates binding energies noticeably and, furthermore, fails to reproduce structure **2**, which is again in line with earlier findings for this particular GGA functional. Additionally, it is worth pointing out that in most structures the moiety angle provided by PBE is too large. TPSS continues to yield the best results in comparison to all other DFT functionals tested concerning both structural parameters (not shown here) and binding energies. It should be mentioned that

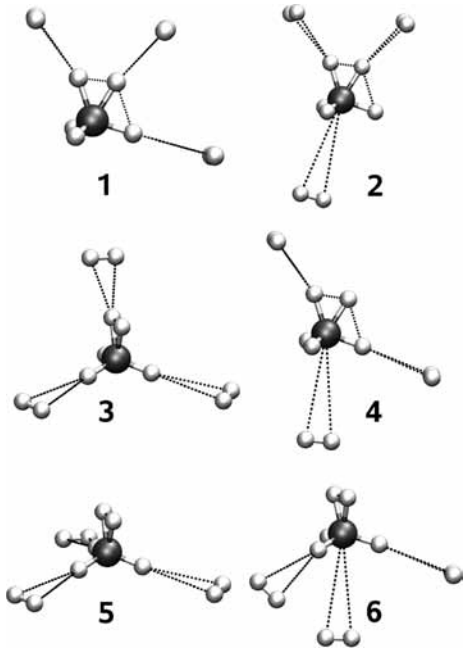

Figure 4. Energetic minima of the $CH_5^+(H_2)_3$ complex. Note: the lines are not intended to denote chemical bonds but only to guide the eye.

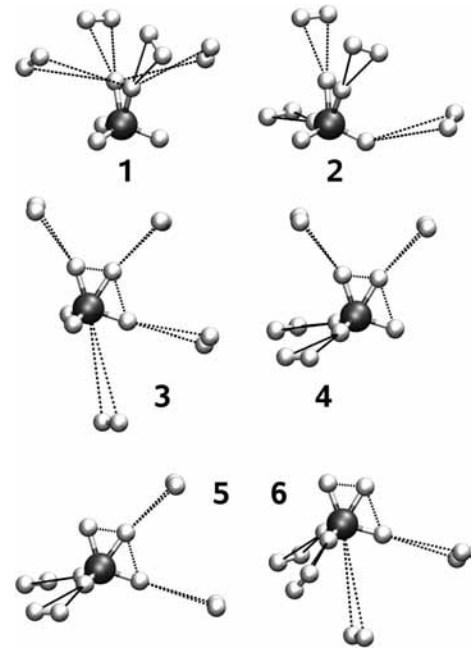

Figure 5. Energetic minima of the $CH_5^+(H_2)_4$ complex. Note: the lines are not intended to denote chemical bonds but only to guide the eye.

TPSS demonstrates the same tendency for binding energies as the one observed for $CH_5^+(H_2)$, namely, it tends to overestimate "strongly bound complexes" by about 0.7−0.3 kcal/mol and to underestimate "weakly bound complexes" by about 0.1−0.3 kcal/mol.

4.2. Larger Complexes: $CH_5^+(H_2)_n$, $n = 3$ and 4. Since we have shown the capability of MP2 to provide good reference values for both structures and binding energies in the cases of $CH_5^+(H_2)$ and $CH_5^+(H_2)_2$, we now assume that MP2 is able to treat larger complexes properly as well. Again, we only display some representative examples in Figures 4 and 5 where we compile the stable structures for $CH_5^+(H_2)_3$ and $CH_5^+(H_2)_4$ complexes, respectively. Analogously to the $CH_5^+(H_2)_2$ case, most of the structures can be constructed using the sites that were already found for $CH_5^+(H_2)$ and $CH_5^+(H_2)_2$; see Figures 1 and 3. So far we have not observed any new sites for $CH_5^+(H_2)_3$, whereas a lot of such structures were generated by the same protocol for the $CH_5^+(H_2)_4$ complex where more H_2 molecules need to be hosted by the CH_5^+ core. We refer the reader to the figures in order to appreciate the wealth of local minima that arises when adding more and more solvating molecules to the CH_5^+ core molecule. For the $CH_5^+(H_2)_3$ complex, we performed the same analysis as in the $n = 2$ case, except we omitted the coupled cluster computations, whereas for the largest complex, only MP2, HF, and TPSS data are shown; see Table 5.

All observations for the $n = 3$ and 4 complexes are rather similar to the ones discussed in the case of $CH_5^+(H_2)_2$. The TPSS results are quite close to the reference values and again the binding energies of "strongly bound complexes" are slightly overpronounced while those of "weakly bound complexes" are slightly underestimated. HF underestimates all binding energies and yields again the wrong order of relative stabilities. As observed before, LDA+B underestimates binding energies dramatically, whereas PBE overestimates them and again cannot reproduce all structures. BLYP also underestimates all binding energies and we observed violations of the correct order of relative stabilities in the $CH_5^+(H_2)_4$ TPSS case. Still, it is again the TPSS functional that yields the best overall performance within the realm of DFT and constitutes by far the best compromise between accuracy and computational effort of all methods considered here.

TABLE 5: Binding Energies of $CH_5^+(H_2)_n$ in kcal/mol, $n = 3$, 4, Computed Using Various Methods

method	1	2	3	4	5	6
			$CH_5^+(H_2)_3$			
MP2	−8.40	−7.81	−6.25	−6.22	−4.56	−3.98
HF	−4.07	−4.17	−3.08	−2.98	−1.70	−1.75
LDA+B	−4.89	−4.40	−3.43	−3.16	−2.06	−1.63
PBE	−10.34	−9.26	−7.70	−7.53	−	−4.35
BLYP	−7.44	−6.69	−5.38	−5.06	−3.59	−2.37
TPSS	−8.94	−8.26	−6.58	−6.46	−4.40	−3.49
			$CH_5^+(H_2)_4$			
MP2	−10.06	−9.72	−9.53	−9.21	−8.02	−5.83
HF	−4.95	−4.71	−4.53	−4.81	−3.32	−1.98
TPSS	−9.45	−9.87	−9.66	−9.57	−8.22	−5.22

5. Conclusions and Outlook

Microsolvation of CH_5^+ by rather weakly interacting H_2 molecules is expected to influence the intramolecular hydrogen scrambling dynamics in the core of $CH_5^+(H_2)_n$ as function of the number of solvent molecules n. This is a dynamical phenomenon taking place on a high-dimensional rugged potential energy surface that is characterized by many quasi-degenerate minima and a wealth of low-lying transition states interconnecting them. In the present investigation we have fairly systematically studied the structures and energetics of $CH_5^+(H_2)_n$ from $n = 1$ up to $n = 4$ using a selection of wave-function-based and density-based electronic structure methods with bare CH_5^+ serving as a well-established reference. It has been shown that MP2 calculations carried out with basis sets of aug-cc-pVQZ or higher quality yield robust reference data when compared to CCSD(T) calculations. For the latter, evidence is provided that single-point calculations based on MP2 structures lead to reliable reference data. With this approach, a large

number of structures has been analyzed, which allowed us to extract characteristic solvation motifs in terms of preferred arrangements of the solvating H_2 molecules.

Furthermore, GGA and meta-GGA density functionals have been checked against the MP2 reference data based on three criteria (quality of structures, binding energies, and scrambling barriers). It must be stressed beforehand that such very weakly bound complexes featuring a multitude of close-lying minima and saddle points on the energy scale of only 0.1−1 kcal/mol (!) are a true challenge for density functional theory; it is noted in passing that the HF approximation fails most badly in all respects. It is found that two popular GGA functionals (BLYP and PBE) and, in particular, the LDA+B combination that very successfully describes bare CH_5^+ fail to describe its microsolvation. Surprisingly, the TPSS meta-GGA functional captures most of the trends upon solvation, including their influence on the hydrogen scrambling barrier in the CH_5^+ core, at a fraction of the cost of the corresponding MP2 or CC calculations. Thus, TPSS is a promising candidate to probe dynamical effects of microsolvation on bare CH_5^+.

Acknowledgment. We are most grateful to Christof Hättig and Arnim Hellweg for advice on carrying out MP2 and CC calculations with Turbomole and Dalton, respectively. This research is in part supported by Deutsche Forschungsgemeinschaft (DFG Normalverfahren: MA 1547/4) and Fonds der Chemischen Industrie (FCI). The calculations were carried out using computational recources of HLRB-II and Bovilab@RUB.

References and Notes

(1) Tal'roze, V. L.; Lyubimova, A. K. *Dokl. Akad. Nauk SSSR* **1952**, *86*, 909.
(2) Kumar P, P.; Marx, D. *Phys. Chem. Chem. Phys.* **2006**, *8*, 573.
(3) Olah, G. A.; Prakash, G. K. S.; Williams, R. E.; Field, L. D.; Wade, K. *Hypercarbon Chemistry*; Wiley: New York, 1987; in particular Chapters 1, 5, and 7.
(4) Olah, G. A. *Angew. Chem., Int. Ed. Engl.* **1995**, *34*, 1393.
(5) Olah, G. A.; Rasul, G. *Acc. Chem. Res.* **1997**, *30*, 245.
(6) Olah, G. A.; Prakash, G. K. S.; Sommer, J. *Superacids*; Wiley: New York, 1985; in particular Chapters 3 and 5.
(7) Oka, T. *Philos. Trans. R. Soc. London, Ser. A* **1988**, *324*, 81.
(8) Asvany, O.; Schlemmer, S.; Gerlich, D. *Astrophys. J.* **2004**, *617*, 685.
(9) Herbst, E. *J. Phys. Chem. A* **2005**, *109*, 4017.
(10) White, E. T.; Tang, J.; Oka, T. *Science* **1999**, *284*, 135.
(11) Marx, D.; Parrinello, M. *Science* **1999**, *284*, 59. See also comment by Kramer, G. M. *Science* **1999**, *286*, 1051a. See response by Oka, T.; White, E. T. *Science* **1999**, *286*, 1051a. See response by Marx, D.; Parrinello, M. *Science* **1999**, *286*, 1051a; www.sciencemag.org/cgi/content/full/286/5442/1051a.
(12) Borman, S. *Chem. Eng. News* **2005**, *83*, 15.
(13) Asvany, O.; Kumar P, P.; Redlich, B.; Hegemann, I.; Schlemmer, S.; Marx, D. *Science* **2005**, *309*, 1219.
(14) Huang, X.; McCoy, A. B.; Bowman, J. M.; Johnson, L. M.; Savage, C.; Dong, F.; Nesbitt, D. J. *Science* **2006**, *311*, 60.
(15) Dyczmons, V.; Kutzelnigg, W. *Theoret. Chim. Acta (Berlin)* **1974**, *33*, 239.
(16) Schleyer, P. v. R.; Carneiro, J. W. de M. *J. Comput. Chem.* **1992**, *13*, 997.
(17) Schreiner, P. R.; Kim, S.-J.; Schaefer, H. F., III; Schleyer, P. v. R. *J. Chem. Phys.* **1993**, *99*, 3716.
(18) Scuseria, G. E. *Nature* **1993**, *366*, 512.
(19) Müller, H.; Kutzelnigg, W.; Noga, J.; Klopper, W. *J. Chem. Phys.* **1997**, *106*, 1863.
(20) Marx, D.; Parrinello, M. *Nature (London)* **1995**, *375*, 216.
(21) Marx, D.; Savin, A. *Angew. Chem., Int. Ed.* **1997**, *36*, 2077.
(22) Kaledin, A. L.; Kunikeev, S. D.; Taylor, H. S. *J. Phys. Chem. A* **2004**, *108*, 4995.
(23) McCoy, A. B.; Braams, B. J.; Brown, A.; Huang, X.; Jin, Z.; Bowman, J. M. *J. Phys. Chem. A* **2004**, *108*, 4991.
(24) Brown, A.; McCoy, A. B.; Braams, B. J.; Jin, Z.; Bowman, J. M. *J. Chem. Phys.* **2004**, *121*, 4105.
(25) Thompson, K. C.; Crittenden, D. L.; Jordan, M. J. T. *J. Am. Chem. Soc.* **2005**, *127*, 4954.
(26) McCoy, A. B. *Int. Rev. Phys. Chem.* **2006**, *25*, 77.
(27) Huang, X.; Johnson, L. M.; Bowman, J. M.; McCoy, A. B. *J. Am. Chem. Soc.* **2006**, *128*, 3478.
(28) Johnson, L. M.; McCoy, A. B. *J. Phys. Chem. A* **2006**, *110*, 8213.
(29) Okulik, N. B.; Peruchena, N. M.; Jubert, A. H. *J. Phys. Chem. A* **2006**, *110*, 9974.
(30) Tian, S. X.; Yang, J. *J. Phys. Chem. A* **2006**, *111*, 415.
(31) Hinkle, C. E.; McCoy, A. B. *J. Phys. Chem. A* **2008**, *112*, 2058.
(32) Hiraoka, K.; Kebarle, P. *J. Am. Chem. Soc.* **1975**, *97*, 4179.
(33) Hiraoka, K.; Mori, T. *Chem. Phys. Lett.* **1989**, *161*, 111.
(34) Hiraoka, K.; Kudaka, I.; Yamabe, S. *Chem. Phys. Lett.* **1991**, *184*, 271.
(35) Boo, D. W.; Lee, Y. T. *Chem. Phys. Lett.* **1993**, *211*, 358.
(36) Boo, D. W.; Liu, Z. F.; Suits, A. G.; Tse, J. S.; Lee, Y. T. *Science* **1995**, *269*, 57.
(37) Boo, D. W.; Lee, Y. T. *J. Chem. Phys.* **1995**, *103*, 520.
(38) Fois, E.; Gamba, A.; Simonetta, M. *Can. J. Chem.* **1985**, *63*, 1468.
(39) Kim, S. J.; Schreiner, P. R.; Schleyer, P. v. R.; Schaefer, H. F., III. *J. Phys. Chem.* **1993**, *97*, 12 232.
(40) Roszak, S.; Leszczynski, J. *Chem. Phys. Lett.* **2000**, *323*, 278.
(41) Ahlrichs, R.; Bär, M.; Häser, M.; Horn, H.; Kölmel, C. Electronic Structure Calculations on Workstation Computers: The Program System TURBOMOLE. *Chem. Phys. Lett.* **1989**, *162*, 165.
(42) Dunning, T. H., Jr. *J. Chem. Phys.* **1989**, *90*, 1007.
(43) *Dalton, a molecular electronic structure program, release 2.0*, 2005. See http://www.kjemi.uio.no/software/dalton/dalton.html.
(44) Helgaker, T.; Jørgensen, P. J.; Olsen, J. *Molecular Electronic-Structure Theory*; Wiley: New York, 2000.
(45) Crespo-Otero, R.; Montero, L. A.; Stohrer, W.-D.; de la Vega, J. M. G. *J. Chem. Phys.* **2005**, *123*, 134107.
(46) van Duijneveldt, F. B.; van Duijneveldt-van de Rijdt, J. G. C. M.; van Lenthe, J. H. *Chem. Rev.* **1994**, *94*, 1873.
(47) Hutter, J.; Alavi, A.; Deutsch, T.; Bernasconi, M.; Goedecker, S.; Marx, D.; Tuckerman, M.; Parrinello, M. *CPMD: Car-Parrinello Molecular Dynamics, version 3.10*; IBM Corp and MPI für Festkörperforschung Stuttgart, 1990−2006; www.cpmd.org.
(48) Perdew, J. P.; Zunger, A. *Phys. Rev. B* **1981**, *23*, 5048.
(49) Becke, A. D. *Phys. Rev. A* **1988**, *38*, 3098.
(50) Lee, C.; Yang, W.; Parr, R. G. *Phys. Rev. B* **1988**, *37*, 785.
(51) Perdew, J. P.; Burke, K.; Ernzerhof, M. *Phys. Rev. Lett.* **1996**, *77*, 3865.
(52) Tao, J.; Perdew, J. P.; Staroverov, V. N.; Scuseria, G. E. *Phys. Rev. Lett.* **2003**, *91*, 146401.
(53) Troullier, N.; Martins, J. L. *Phys. Rev. B* **1991**, *43*, 1993.
(54) Helgaker, T.; Gauss, J.; Jørgensen, P.; Olsen, J. *J. Chem. Phys.* **1997**, *106*, 6430.
(55) Coriani, S.; Marchesan, D.; Gauss, J.; Hättig, C.; Helgaker, T.; Jørgensen, P. *J. Chem. Phys.* **2005**, *123*, 184107.

JP8054069